

NON-LINEAR MULTIMODE RESPONSE OF CLAMPED RECTANGULAR PLATES TO ACOUSTIC LOADING

Chuh Mei
Old Dominion University

and

Donald B. Paul
Air Force Wright Aeronautical Laboratories

AD-P003 690

1. INTRODUCTION

Acoustically induced fatigue failures in aircraft structural components have resulted in unacceptable maintenance and inspection burdens. In some cases, sonic fatigue failures have resulted in major structural redesigns. Therefore, accurate prediction methods are needed to determine the sonic fatigue life of structures.

Many analytical and experimental programs to develop sonic fatigue design criteria, however, have repeatedly shown a poor comparison between analytical and measured maximum root-mean-square (RMS) strain at high sound pressure levels. [1,2]. Deviations in excess of 100 percent are common. Neglecting large-deflections in the analysis has been identified as a major reason for the enormous discrepancy [2]. Recently, analytical efforts [3,4] with a single-mode approach, and a test program [5] have demonstrated that the prediction of panel random response is greatly improved by including the large-amplitude effect in the formulation. Test results [5] also show that there is more than one mode responding. Multiple modes were also observed by White [6] in experimental studies on aluminum and carbon fiber-reinforced plates under acoustic loading. White also showed that the fundamental mode responded significantly and contributed more than one-half of the total mean-square strain response. Therefore, in order to have an accurate determination of the random response of a structure, multiple modes should be used in the analysis. This paper presents an analytical solution technique for the large-amplitude random response of clamped rectangular plates considering multiple modes in the analysis. The von Kármán large-deflection plate equations are solved by a technique which reduces the fourth order nonlinear partial differential equations to a set of second order nonlinear differential equations with time as the independent variable. A Fourier-type series representation of the out-of-plane deflection and stress function is assumed. The compatibility equation is solved by direct substitution, and the equilibrium equation is solved through the use of Bubnov-Galerkin approach. The acoustic excitation is assumed to be Gaussian. The Krylov-Bogoliubov-Cauchey equivalent linearization method [7,9] is then used so that the derived set of second order nonlinear differential equations are linearized to an equivalent set of second order linear differential equations. Transformation of coordinates from the generalized displacements to the normal-mode coordinates, and an iterative scheme are employed to obtain RMS maximum panel deflection, RMS maximum strain, and equivalent linear (or nonlinear) frequencies for rectangular plates at various excitation pressure spectral densities. Convergence of the results is demonstrated by using 4, 6, 10, and 15 terms in the transverse deflection function.

2. MATHEMATICAL FORMULATION AND SOLUTION PROCEDURE

Assuming that the effects of both inplane and rotatory inertia forces can be neglected, the dynamic von Kármán equations of a rectangular isotropic

plate are

$$L(w, F) = D\nabla^4 w + phw_{,tt} + gw_{,t} - p(t) - h(F_{,yy}w_{,xx} + F_{,xx}w_{,yy} - 2F_{,xy}w_{,xy}) = 0 \quad (1)$$

$$\nabla^4 F = E(w_{,xy}^2 - w_{,xx}w_{,yy}) \quad (2)$$

The transverse deflection which satisfies the clamped boundary conditions

$$w = w_{,x} = 0 \quad \text{on } x = 0 \text{ and } a \quad (3a)$$

$$w = w_{,y} = 0 \quad \text{on } y = 0 \text{ and } b \quad (3b)$$

is assumed as

$$w(y, t) = h \sum_m \sum_n W_{mn}(t) f_m(x) g_n(y) \quad m, n = 1, 2, 3, \dots \quad (4)$$

where

$$f_m(x) = \cos \frac{(m-1)\pi x}{a} - \cos \frac{(m+1)\pi x}{a} \quad (5)$$

$$g_n(y) = \cos \frac{(n-1)\pi y}{b} - \cos \frac{(n+1)\pi y}{b} \quad (6)$$

Upon examination of the foregoing expression for the transverse deflection, it is found that the compatibility equation (2) can be identically satisfied if the stress function F is taken in the following form:

$$F = -P_x \frac{y^2}{2} - P_y \frac{x^2}{2} + Eh^2 \sum_p \sum_q F_{pq} \cos \frac{p\pi x}{a} \cos \frac{q\pi y}{b} \quad p, q = 0, 1, 2, \dots \quad (7)$$

Direct substitution of Eqs. (4) and (7) into Eq. (2), performing the required differentiations, multiplications, and a Fourier analysis of the resulting terms yields a quadratic relationship between F_{pq} and W_{mn}

$$F_{pq} = \frac{1}{(p^2/\alpha + q^2\alpha)^2} \sum_m \sum_n \sum_k \sum_l B_{pqmnkl} W_{mn} W_{kl} \quad (8)$$

in which B_{pqmnkl} are integers (tabulated in Reference 10) and $\alpha = a/b$. A complete description of the solution technique used to solve equation (2) is given in Reference [10].

The average edge loads P_x and P_y in Eq. (7) are determined from inplane boundary conditions. The particular inplane boundary condition of most interest in the study of sonic fatigue of structural panels is the one in which the edges are restrained from movement, that is

$$u=0 \quad \text{on } x=0 \text{ and } a \quad (9a)$$

$$v=0 \quad \text{on } y=0 \text{ and } b \quad (9b)$$

or

$$\int_0^a \frac{\partial u}{\partial x} dx = \int_0^a \left[\frac{1}{E} (F_{,yy} - v F_{,xx}) - \frac{1}{2} w_{,x}^2 \right] dx = 0 \quad (10a)$$

$$\int_0^b \frac{\partial v}{\partial y} dy = \int_0^b \left[\frac{1}{E} (F_{,xx} - v F_{,yy}) - \frac{1}{2} w_{,y}^2 \right] dy = 0 \quad (10b)$$

Performing the differentiation and integration as indicated in Eq. (10) yields relationships for P_x and P_y in terms of the deflection coefficients w_{mn} . These relations are too lengthy to reproduce here, but may be found in References [10] and [11].

With the assumed deflection w given by Eq. (4) and the stress function F given by Eq. (7), Eq. (1) is then satisfied by applying Bubnov-Galerkin method:

$$\iint L(w, F) f_r g_s dx dy = 0 \quad r, s = 1, 2, 3, \dots \quad (11)$$

The integration of each of the terms in Eq. (11) can be found in Ref. [10]. A set of nonlinear time-differential equations is obtained after performing the integration over the total area of the panel, and it can be written in matrix notation as

$$[M]\{\ddot{W}\} + [C]\{\dot{W}\} + [K]_L\{W\} + \{\beta(W)\} = \{p(t)\} \quad (12)$$

where $[M]$, $[C]$, and $[K]_L$ are the generalized mass, damping, and linear stiffness matrices, respectively, and $\{\beta\}$ is a vector function which is cubic in the generalized displacements $\{W\}$.

If the acoustic pressure excitation $p(t)$ is stationary Gaussian, ergodic, and has a zero mean, then application of the Krylov-Bogoliubov-Caughey equivalent linearization technique [3,4,7-9] yields an equivalent set of linear equations as

$$[M]\{\ddot{W}\} + [C]\{\dot{W}\} + ([K]_L + [K]_{EL})\{W\} = \{p(t)\} \quad (13a)$$

or

$$[M]\{\ddot{W}\} + [C]\{\dot{W}\} + [K]\{W\} = \{p(t)\} \quad (13b)$$

The elements of the generalized equivalent linear or nonlinear stiffness matrix $[K]_{EL}$ can be derived from the expression [8]

$$(K_{EL})_{rsij} = \epsilon \left[\frac{\partial \beta_{rs}}{\partial w_{ij}} \right] \quad (14)$$

where $\xi\{\}$ is an expected value operator. The elements $(K_{EL})_{rsij}$ are too lengthy to reproduce here, but may be found in Reference [11]. The approximate generalized displacements $\{W\}$, computed from the linearized Eq. (13), are also Gaussian and approach stationary because the panel motion is stable.

To determine the mean-square generalized displacements $\overline{W_{mn}^2}$ an iterative process is introduced. The undamped linear equation of Eq. (13a) is solved first, which required simply the determination of the eigenvalues and eigenvectors of the undamped linear equation

$$\omega_j^2 [M]\{\phi\}_j = [K]_L\{\phi\}_j \quad (15)$$

where ω_j is the linear frequency of vibration, and $\{\phi\}_j$ is the normal mode shape.

Apply a coordinate transformation, from the generalized displacements to the normal coordinates (this analysis will use the first 4 modes), by

$$\begin{matrix} \{W\} &= & [\phi] & \{q\} & & 4 \times m \\ m \times 1 & & m \times 4 & 4 \times 1 & & \end{matrix} \quad (16)$$

where each column of $[\phi]$ is a normal mode $\{\phi\}_j$. The damped linear equation of Eq. (13a) becomes

$$[M]\{\ddot{q}\} + [C]\{\dot{q}\} + [K]_L\{q\} = \{P(t)\} \quad (17)$$

where

$$[M] = [\phi]^T [M] [\phi] \quad (18a)$$

$$[C] = [\phi]^T [C] [\phi] = 2[\zeta\omega][M] \quad (18b)$$

$$[K]_L = [\phi]^T [K]_L [\phi] = [\omega^2][M] \quad (18c)$$

$$\{P\} = [\phi]^T \{p\} \quad (18d)$$

The j th row of Eq. (17) is

$$\ddot{q}_j + 2\zeta_j \omega_j \dot{q}_j + \omega_j^2 q_j = \frac{P_j}{M_j} \quad (19)$$

The mean-square normal coordinate is simply

$$\overline{q_j^2} \approx \frac{\pi S_p(\omega_j)}{4M_j^2 \zeta_j \omega_j^3} \quad (20)$$

where $S_p(\omega)$ is the spectral density function of the excitation $P_j(t)$. The covariance matrix of the linear generalized displacements is

$$\overline{[W_{mn} W_{kl}]}_L = \frac{\pi}{4} \int (\phi)_j \frac{S_p(\omega_j)}{M_j^2 \zeta_j \omega_j^3} (\phi)_j^T \quad (21)$$

This initial estimate of expected value on generalized displacements can now be used to compute the generalized linear stiffness matrix $[K]_{EL}$ through Eq.

(14). The undamped linearized equation of Eq. (13) is solved again

$$\Omega_j^2 [M] \{\phi\}_j = ([K]_L + [K]_{EL}) \{\phi\}_j \quad (22)$$

where Ω_j is the equivalent linear or nonlinear frequency of vibration, and $\{\phi\}_j$ is the associated equivalent linear normal mode shape. Then Eq. (13) is transformed again and has the form as

$$[M] \{\ddot{q}\} + [C] \{\dot{q}\} + [K] \{q\} = \{P(t)\} \quad (23)$$

in which

$$[K] = [\phi]^T ([K]_L + [K]_{EL}) [\phi] = [\Omega^2] [M] \quad (24)$$

the j th row of Eq. (23) is

$$\ddot{q}_j + 2\zeta_j \omega_j \dot{q}_j + \Omega_j^2 q_j = \frac{P_j}{M_j} \quad (25)$$

and the displacement covariance matrix is

$$\overline{[W_{mn} W_{kl}]} = \frac{\pi}{4} \int (\phi)_j \frac{S_p(\Omega_j)}{M_j^2 \zeta_j \omega_j^3} (\phi)_j^T \quad (26)$$

The diagonal terms of $\overline{[W_{mn} W_{kl}]}$ are the mean-square generalized displacements $\overline{W_{mn}^2}$. As the iterative process converges on the iter-th cycle, the relations

$$(\overline{q_j^2})_{iter} \approx (\overline{q_j^2})_{iter-1} \quad (27a)$$

$$(\overline{\Omega_j^2})_{iter} \approx (\overline{\Omega_j^2})_{iter-1} \quad (27b)$$

$$(\overline{W_{mn}^2})_{iter} \approx (\overline{W_{mn}^2})_{iter-1} \quad (27c)$$

become satisfied. Convergence is considered achieved when the difference of the RMS displacements satisfies the requirement

$$\left| \frac{(\text{RMS } W_{mn})_{iter} - (\text{RMS } W_{mn})_{iter-1}}{(\text{RMS } W_{mn})_{iter}} \right| < 10^{-3} \text{ for all } m, n \quad (28)$$

Once the RMS generalized displacements are determined, the RMS deflection and the maximum RMS strain can be determined from Eqs. (4), (7) and the strain-displacement relations as follows.

For a rectangular plate ($a \geq b$) with clamped support along all four edges, the maximum bending strain occurs at the extreme-fiber perpendicular to its long edge at the midpoint.

$$(\epsilon_y)_b = \pm \frac{h}{2} \frac{\partial^2 w}{\partial y^2} \quad (29a)$$

or

$$\left(\frac{\epsilon_y b^2}{h^2}\right)_b = \pm \frac{\pi^2}{2} \sum_{mn} f_m(x) \left[(n-1)^2 \cos \frac{(n-1)\pi y}{b} - (n+1)^2 \cos \frac{(n+1)\pi y}{b} \right] W_{mn} \quad (29b)$$

The membrane strain is given by

$$(\epsilon_y)_m = \frac{1}{E} (F_{,xx} - \nu F_{,yy}) \quad (30a)$$

or

$$\left(\frac{\epsilon_y b^2}{h^2}\right)_m = \frac{\pi^2}{8} \sum_{mn} W_{mn} Z_y(W_{mn}) + \sum_{mnklpq} C_{pq} B_{pqmnkl} W_{mn} W_{kl} \quad (30b)$$

in which

$$C_{pq} = \frac{\pi^2 (\nu q^2 - p^2/a^2)}{(p^2/a + q^2/a)^2} \cos \frac{p\pi x}{a} \cos \frac{q\pi y}{b} \quad (31)$$

From

$$\epsilon_y = (\epsilon_y)_b + (\epsilon_y)_m \quad (32)$$

the maximum mean-square strain becomes

$$\overline{\left(\frac{\epsilon_y b^2}{h^2}\right)^2} = \overline{\left(\frac{\epsilon_y b^2}{h^2}\right)_b^2} + 2 \overline{\left(\frac{\epsilon_y b^2}{h^2}\right)_b \left(\frac{\epsilon_y b^2}{h^2}\right)_m} + \overline{\left(\frac{\epsilon_y b^2}{h^2}\right)_m^2} \quad (33)$$

For Gaussian random processes with zero-mean we have

$$\xi(W_{ij} W_{kl} W_{mn}) = 0 \quad (34)$$

$$\begin{aligned} \xi(W_{ij} W_{kl} W_{mn} W_{rs}) &= \xi(W_{ij} W_{kl}) \xi(W_{mn} W_{rs}) \\ &+ \xi(W_{ij} W_{mn}) \xi(W_{kl} W_{rs}) + \xi(W_{ij} W_{rs}) \xi(W_{kl} W_{mn}) \end{aligned} \quad (35)$$

and the maximum RMS strain can be determined from Eq. (33).

3. RESULTS AND DISCUSSION

Using the present formulation, the nonlinear response of square and rectangular ($\alpha=2$) plates with all edges clamped and subjected to broadband random excitation are studied. In the results presented, the white noise excitation is band-limited with a frequency bandwidth of 25 Hz to 6000 Hz, the damping ratio is assumed to be constant for all four normal modes and Poisson's ratio is equal to 0.3. Mean-square center deflection and maximum mean-square strain are presented in a nondimensional form. The nondimensional forcing spectral density parameter is defined as

$$S_f = \frac{2\pi S_p(\omega)}{\rho^2 h^4 \left(\frac{D}{\rho h b^4}\right)^{3/2}} \quad (36)$$

Also, since the loading is symmetric, only symmetric generalized displacements W_{mn} are retained in the transverse deflection function.

The convergence of the solution technique was examined in order to determine the degree of accuracy possible with a highly truncated transverse deflection function series. The mean-square center deflection versus the non-dimensional spectral density parameter using 4, 6, 10, and 15 terms in the deflection function for a square plate is shown in Figure 1. The particular generalized displacements that make up the various orders of the deflection function are shown in Table 1. Figure 1 clearly indicates that a 6-term solution gives accurate results for the nonlinear maximum deflection while a 4-term solution will provide accurate linear results. The maximum strain occurs at the extreme fiber of the panel and at the midpoint of the long edge. The direction is perpendicular to the edge. Figure 2 shows the maximum mean-square strain versus S_f for the square plate using 4, 6, 10 and 15 terms in the deflection function. The convergence of the mean-square strain is much slower as compared with that of the mean-square deflection.

TABLE I
Generalized Displacements Used in Convergence Studies

Number of terms	Generalized Displacements															
	W_{11}	W_{13}	W_{31}	W_{33}	W_{55}	W_{51}	W_{35}	W_{53}	W_{17}	W_{71}	W_{55}	W_{37}	W_{73}	W_{19}	W_{91}	
4	X	X	X	X												
6	X	X	X	X	X	X										
10	X	X	X	X	X	X	X	X	X	X						
15	X	X	X	X	X	X	X	X	X	X	X	X	X	X	X	

Figures 3 and 4 show the maximum mean-square nondimensional deflection versus the nondimensional spectral density of acoustic pressure excitation for rectangular panels of aspect ratios of 1 and 2 with the damping ratio equal to 0.009, 0.018 and 0.027. Figures 5 and 6 show the maximum nondimensional mean-square strain versus the nondimensional spectral density for rectangular panels of aspect ratios of 1 and 2 with the damping ratio

equal to 0.009, 0.018 and 0.027. Ten terms were included in the deflection function, to generate the results shown in Figures 3 through 6.

4. CONCLUDING REMARKS

An analytical solution technique is presented for determining the large-amplitude random response of clamped rectangular panels while including multiple modes in the analysis. Accurate mean-square deflections can be obtained with the use of 6 terms in the deflection function, while it is necessary to consider as many as 10 or more terms for the accurate determination of the strains. In the numerical examples presented, a constant damping ratio for all four modes has been used. However, nonlinear damping phenomena have been observed in experiments [5,6]. Therefore, further effort, is needed to better understand the effects of nonlinear damping on panel response.

5. REFERENCES

1. I. HOLEHOUSE 1980 Sonic Fatigue Design Techniques for Advanced Composite Aircraft Structures, "AFWAL-TR-79-3028, AF Flight Dynamics Laboratory, WPAFB, OH.
2. C. MEI 1979 Large Amplitude Response of Complex Structures due to High Intensity Noise, AFFDL-TR-79-3028, AF Flight Dynamics Laboratory, WPAFB, OH.
3. C. MEI 1980 Response of Nonlinear Structural Panels Subjected to High Intensity Noise, AFWAL-TR-80-3018, AF Wright Aeronautical Laboratories, WPAFB, OH.
4. C. MEI, D. B. PAUL and K. R. WENTZ 1982 Large Amplitude Random Response of Symmetric Laminated Composite Plates. Shock and Vibration Bulletin, Bulletin 52, pp. 99-111.
5. C. MEI and K. R. WENTZ 1982 Analytical and Experimental Nonlinear Response of Rectangular Panels to Acoustic Excitation. 23rd Structures, Structural Dynamics and Materials Conference. New Orleans, LA. pp. 514-520.
6. R. G. WHITE 1978 Comparison of the Statistical Properties of the Aluminum Alloy and CFRP Plates to Acoustic Excitation. J. Composites. pp. 251-258.
7. W. D. IWAN and P. T. D. SPANOS 1978 On the Existence and Uniqueness of Solutions Generated by Equivalent Linearization. Int. J. Nonlinear Mech., Vol. 13. pp. 71-78.
8. T. S. ATALIK and S. UTKU 1976 Stochastic Linearization of Multi-Degree-of-Freedom Nonlinear Systems. Earthquake Eng. Struct. Dyn. Volume 4. pp. 411-420.
9. T. K. CAUGHEY 1971 Nonlinear Theory of Random Vibrations in Advances in Applied Mechanics, Edited by C. S. Yih, Vol. 11, Academic Press. pp. 209-253.
10. D. B. PAUL 1980 Ph.D Thesis, The Ohio State University. Large Deflections of Clamped Rectangular Plates with Arbitrary Temperature Distributions.
11. C. MEI 1983 AF Wright Aeronautical Laboratories, AFWAL-TR-83-3121. Large Deflection Multimode Response of Clamped Rectangular Panels to Acoustic Excitation.

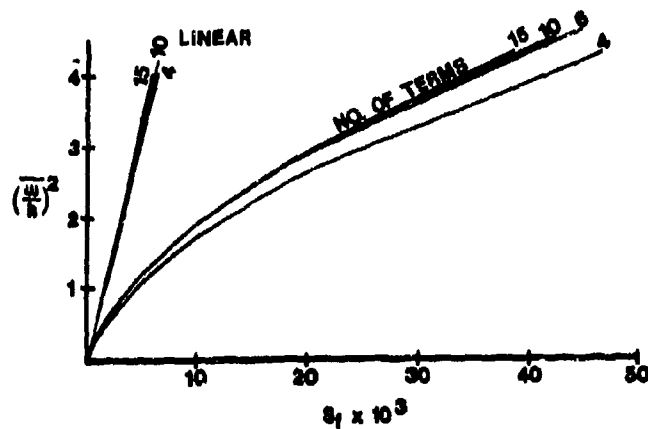


Figure 1. Convergence of the Mean-Square Center Deflection for the Square Plate ($\xi = 0.009$)

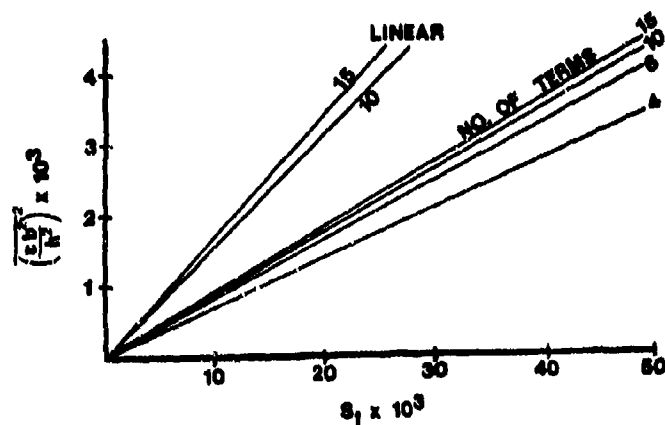


Figure 2. Convergence of the Maximum Mean-Square Strain for the Square Plate ($\xi = 0.009$)

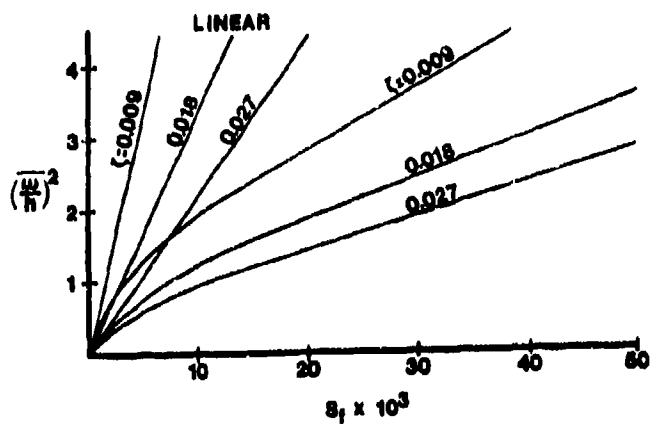


Figure 3. Mean-Square Center Deflection vs Pressure Spectral Density for a Clamped Square Plate

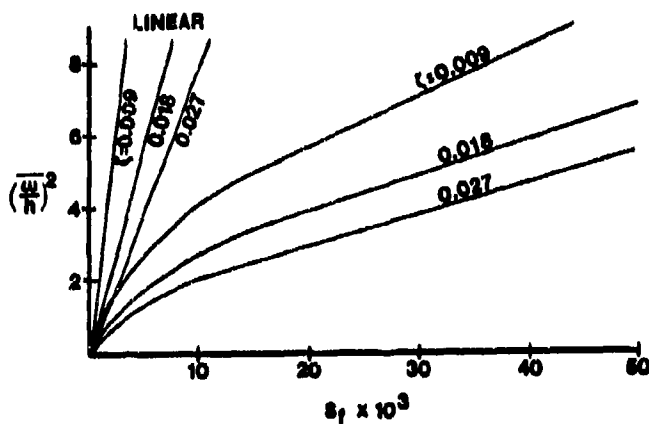


Figure 4. Mean-Square Center Deflection vs Pressure Spectral Density for a Clamped Rectangular ($\alpha = 2$) Plate

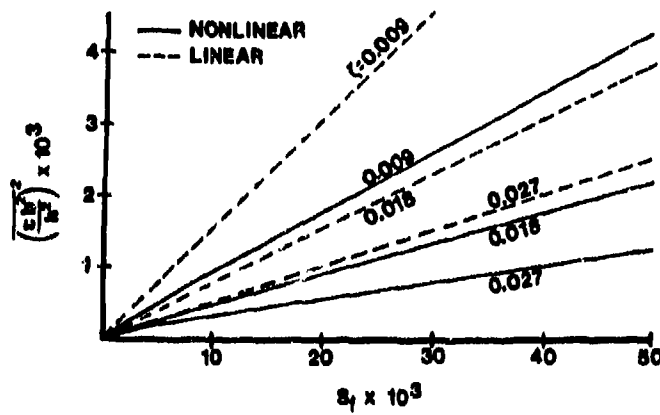


Figure 5. Maximum Mean-Square Strain
vs Pressure Spectral Density
for a Clamped Square Plate

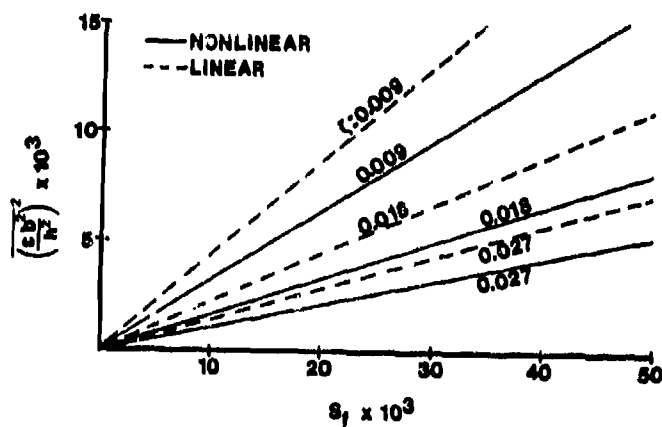


Figure 6. Maximum Mean-Square Strain
vs Pressure Spectral Density
for a Clamped Rectangular
($\alpha = 2$) Plate



10. RESPONSE TO SEISMIC EXCITATION